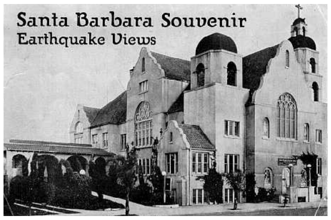

4th IASPEI / IAEE International Symposium:

Effects of Surface Geology on Seismic Motion

August 23–26, 2011 · University of California Santa Barbara

SEISMIC MICROZONATION AND DEVELOPMENT OF SEISMIC DESIGN GROUND MOTIONS FOR THE STANFORD UNIVERSITY CAMPUS, CALIFORNIA

Ivan Wong and Patricia Thomas
Seismic Hazards Group
URS Corporation
Oakland, CA 94612
USA

Fouad Bendimerad
RET International
125-B 24th Avenue
San Mateo, CA 94403
USA

Walt Silva and Nick Gregor
Pacific Engineering & Analysis
856 Seaview Drive
El Cerrito, CA 94530
USA

Kenneth Stokoe and Jiabei Yuan
Civil Engineering-Geotechnical
University of Texas at Austin
Austin, TX 78712
USA

ABSTRACT

Stanford University is located in the seismically active San Francisco Bay area adjacent to the San Andreas fault. The University commissioned a multi-disciplinary team to update the seismic hazard evaluation and revise the campus-wide design ground motions. A campus-wide probabilistic seismic hazard analysis was performed and deterministic scenario ground motions also were calculated to compare with the probabilistic ground motions. Spectral-analysis-of-surface-waves (SASW) surveys were performed at 15 locations and the resulting V_S data were used to microzone the campus based on site response analyses and the distance to the San Andreas fault. Site response analyses were performed to incorporate the effects of the near-surface geology beneath the campus into the design ground motions. One-dimensional analyses were performed using a RVT-equivalent-linear approach for both the north-central and east campus using the 475-year and 2,475-year return period probabilistic ground motions and the 84th percentile deterministic spectra for a firm soil site condition as input ground motions. Site-specific Design Response Spectra following ASCE 7-05 and the recently developed ASCE 7-10 and Basic Safety Earthquake (BSE)-1 (10% in 50 years) and BSE-2 (2% in 50 years) spectra consistent with ASCE 41-06 were developed.

INTRODUCTION

Stanford University is located in the seismically active San Francisco Bay region within the San Andreas fault system (Figs. 1 and 2). The west side of campus is located about 6 km from the San Andreas fault, which last ruptured in the 1906 moment magnitude (**M**) 7.9 "Great San Francisco" earthquake. The site of the campus was also shaken in the 1838 **M** 6.8 San Francisco Peninsula earthquake and $120 million (1989 dollars) of damage was incurred in the 1989 **M** 6.9 Loma Prieta

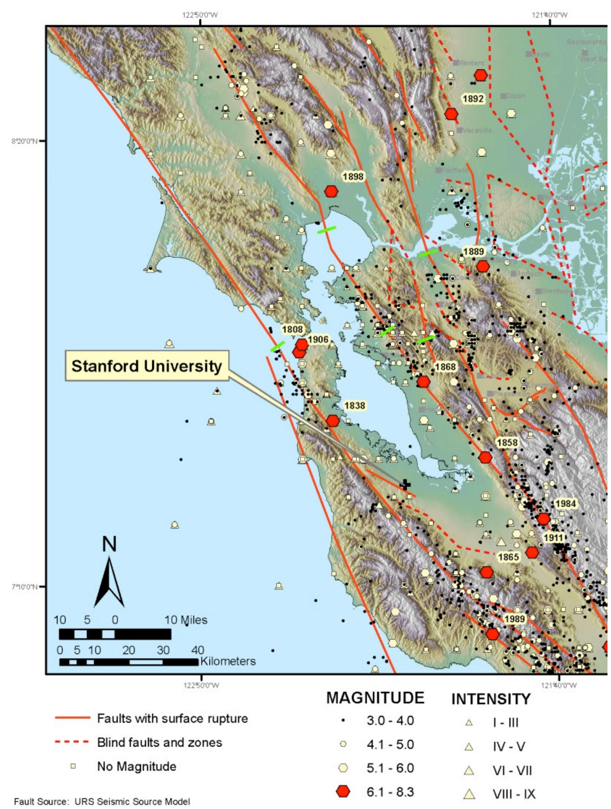

Fig. 1. Historical seismicity in the San Francisco Bay region (M ≥ 3.0) 1800-2007.

earthquake. This paper describes the process and provides key results of the update of the seismic hazard evaluation of the campus and the campus-wide design ground motions.

In an earlier 2008 study (Wong *et al*., 2008a), the seismic design ground motions for the campus were recognized as being conservative because it was intended to cover a wide range of soil conditions that were not well constrained due to the lack of any site-specific shear-wave velocity (V_S) data for the campus. In this study, spectral-analysis-of-surface-waves (SASW) surveys were performed at 15 locations on campus and the resulting V_S data were used to microzone the campus based on site response analyses and the distance to the San Andreas fault.

An objective of this study was to estimate the levels of ground motions at a specified exceedance probability based upon a probabilistic seismic hazard analysis (PSHA). Deterministic scenario ground motions also were calculated to compare with the probabilistic ground motions. A site response analysis was performed to incorporate the effects of the near-surface geology beneath the campus into the design ground motions. Seismic design ground motions following the standards of ASCE 7-05 *Minimum Design Loads for Building and other Structures* and ASCE 41-06 *Seismic Rehabilitation of Existing Buildings* were developed. Specifically, site-specific Design Response Spectra (DRS) following ASCE 7-05 and the recently developed ASCE 7-10, e.g., use of the maximum component and Basic Safety Earthquake (BSE)-1 (10% in 50 years) and BSE-2 (2% in 50 years) spectra consistent with ASCE 41-06 were developed.

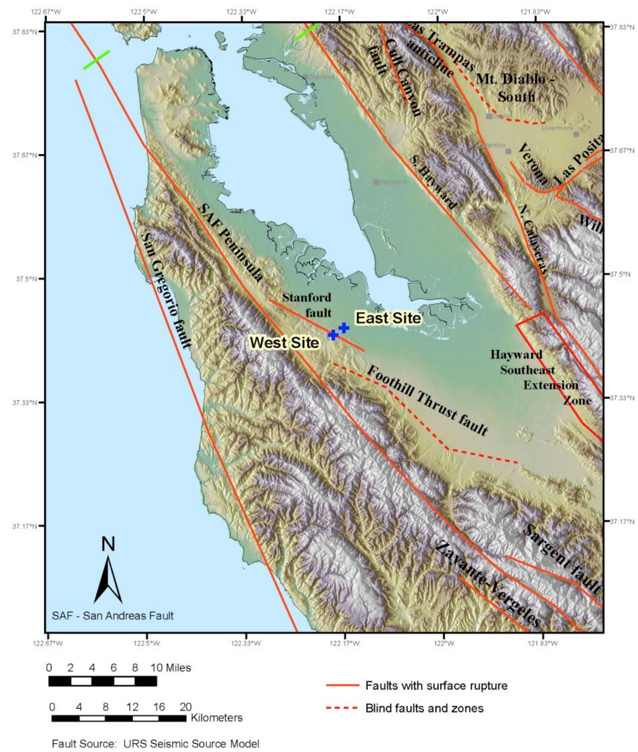

Fig. 2. Active faults in the vicinity of the campus.

SASW SURVEYS AND MICROZONATION

SASW surveys were performed on the Stanford University campus from 2 to 7 August 2009 (Table 1; Fig. 3). The surveys were performed by personnel from the University of Texas at Austin.

Table 1. SASW Sites, Their V_S30 and NEHRP Site Classes

Location	V_S30 (m/sec)	Campus Zone	NEHRP Site Class
Abram's Court	274	North-Central	D
Arboretum Road	325	East	D
Children's Center	294	East	D
Electioneer Road	376	West	C
Enchanted Broccoli Forest	295	North-Central	D
Equestrian Center	328	West	D
Escondido Mall	351	North-Central	D
Foothills	400	West	C
Manzanita Fields	329	North-Central	D
New Concert Hall	315	East	D
Parking Structure #1	336	East	D
Roble Field	328	North-Central	D
Sand Hill Fields	372	North-Central	C
The Oval	321	East	D
Wilbur Hall	307	North-Central	D

NEHRP Site Class V_S30

A	> 1,524 m/sec	D	183 to 366 m/sec
B	762 to 1,524 m/sec	E	< 183 m/sec
C	366 to 762 m/sec		

Fig. 3. SASW surveys: (a) Thumper, (b) survey at the Children's Center, and (c) Y1100 vibroseis.

The SASW method is a nondestructive and nonintrusive seismic method (Stokoe *et al*., 1994) involves generating seismic surface waves at one point on the ground and measuring at multiple surface locations the ground motions created by the passage of the surface waves. Three measurement locations are typically used with each source location. Ground motions were measured using 1 Hz seismometers.

For short measurement spacings, a sledge hammer was used for the source of the surface waves. For longer spacings (> 7.5 m), testing was performed using the vibrator trucks called "Thumper" or the Y1100, a vibroseis previously owned by CONOCO and used in petroleum exploration (Fig. 3). Thumper was developed as part of the National Earthquake Engineering Simulation (NEES) Program funded by the National Science Foundation.

The survey locations are shown on Fig. 4. The resulting V_S profiles are shown in Fig. 5. The V_S profiles show similar trends except for three profiles in the west campus area: the Foothills, Equestrian Center, and Electioneer Road (Fig. 4), which exhibit strong velocity contrasts at depth indicating the presence of rock (V_S > 2,500 ft/sec) (Fig. 5).

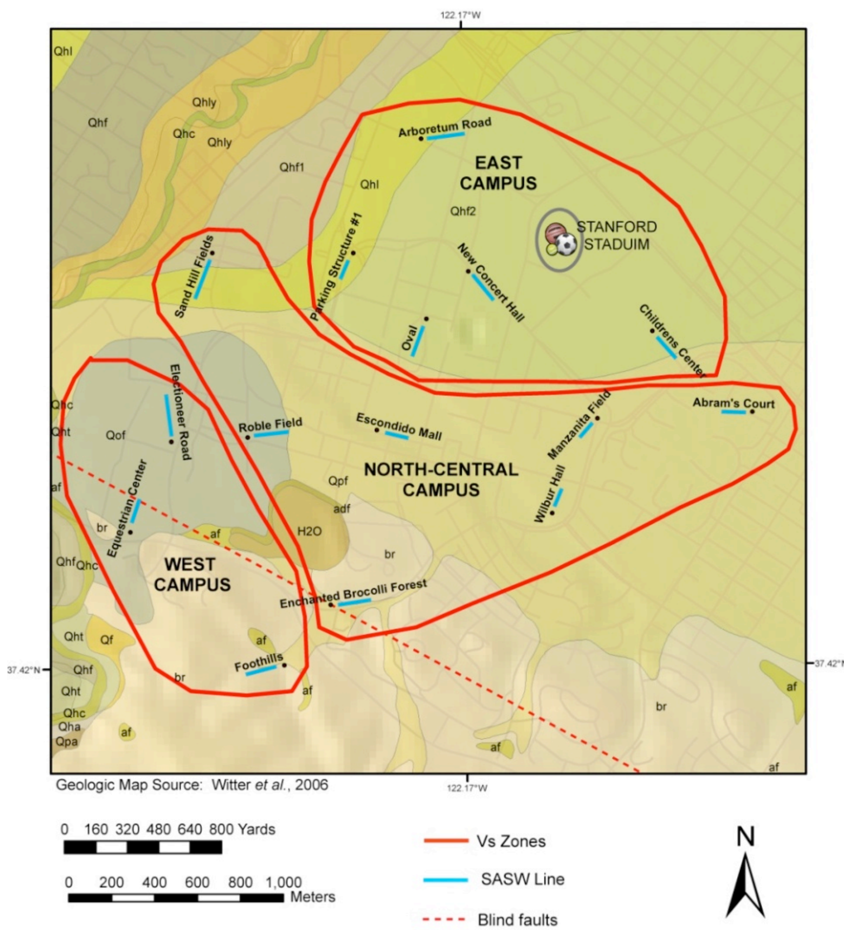

Fig. 4. SASW survey locations, Quaternary geology, and campus zones.

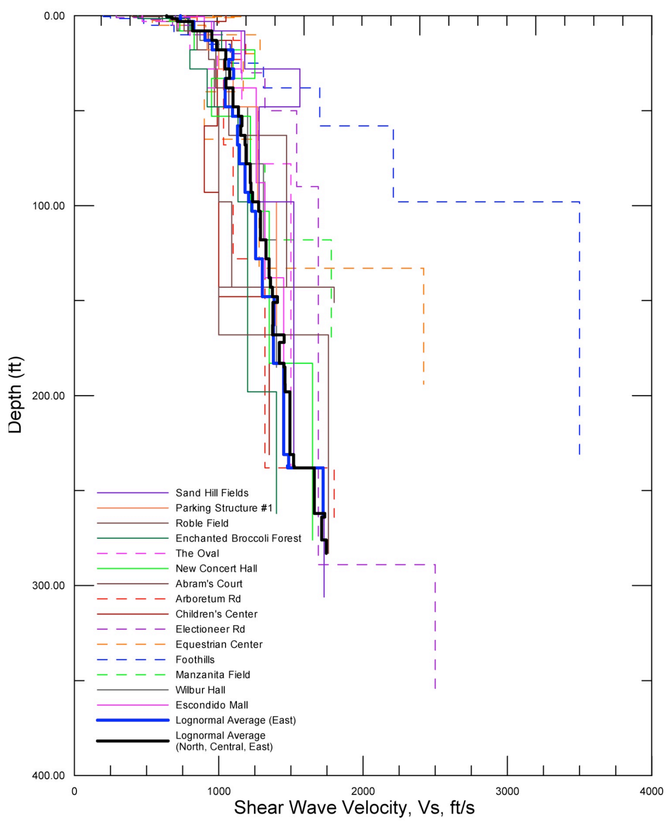

Fig. 5. All SASW V_S profiles and the north-central and east campus basecase profiles.

Because of the relatively thin soil site conditions, design ground motions for the west campus (Fig. 4) were not developed in this study. Future site-specific studies will be required for any site in the west campus due to anticipated strong amplification effects on ground motions.

The remaining V_S profiles were examined to see if they could be grouped together geographically based on similarities in their profiles and near-surface geology. The most obvious groupings were sites on the north-central campus and east campus based on the V_S profiles (Fig. 4). The north-central campus V_S profiles were, in general, faster (stiffer) than the east campus. We also considered the division of the V_S profiles into two groups based on the surficial geologic map of Witter *et al.* (2006): (1) north-central campus where the sites are generally situated on late Pleistocene alluvial fan deposits (Qpf) and early to mid-Pleistocene alluvial fan and stream terrace deposits (Qof) and (2) east campus where Holocene floodplain deposits (Qhf2) and Holocene natural levee deposits (Qhl) are the predominant units (Fig. 4).

Base case V_S profiles were computed for the north-central campus and east campus by computing a lognormal mean of the grouped profiles. (The "base case" profiles are used in the profile randomization.) A comparison of the base case V_S profiles for the two campus areas is shown on Fig. 5. Despite apparent differences in the V_S profiles in each zone, the north-central and east base case V_S profiles are quite similar.

Since the SASW data did not reach rock beneath the north-central and east campuses, the depth to a rock-like V_S of 3,280 ft/sec (1 km/sec) was varied in the site response analyses consistent with the NGA models use of $Z_{1.0}$. The V_S of 3,280 ft/sec is also a rough average of the rock V_S encountered at the three sites in west campus (Fig. 5). At Electioneer Road, rock ($V_S > 2{,}500$ ft/sec) was encountered at a depth of 290 ft. To the west at the Foothill site, rock ($V_S > 3{,}500$ ft/sec) was shallower as expected at a depth of about 100 ft (Fig. 5). Hence, we varied the depth to rock (V_S 3,280 ft/sec) using values of 300, 350, 400, and 500 ft since we expect rock to be at a depth of about 300 ft as observed at Electioneer Road or deeper.

A V_S30 (average shear-wave velocity in the top 30 m) value was computed for each site from its V_S profile and a NEHRP site class assigned (Table 1). These site classes can be used for code-based design if deemed appropriate.

PROBABILISTIC SEISMIC HAZARD ANALYSIS

In this study, the available geologic and seismologic data were used to evaluate and characterize: (1) potential seismic sources, (2) the likelihood of earthquakes of various magnitudes occurring on those sources, and (3) the likelihood of the earthquakes producing ground motions over a specified level. The PSHA approach used in this study is based on the model developed principally by Cornell (1968). The calculations were made using the computer program HAZ38 developed by Norm Abrahamson. The program has been validated in the Pacific Earthquake Engineering Research (PEER) Center-sponsored "Validation of PSHA Computer Programs" Project (Thomas *et al*., 2010).

The campus is located 6 km from the San Andreas fault, about 23 km from the San Gregorio fault, and approximately 24 km from the Hayward fault, all of which are capable of generating large ($\mathbf{M} \geq 7$) earthquakes. In addition to these major faults, there are numerous subsidiary, active faults within 50 km of the site, including the Stanford fault zone, which underlies the campus (Figs. 1 and 2). A total of 15 earthquakes of $\mathbf{M} \geq 6.0$ have occurred in the San Francisco Bay region since (1850) (Fig. 1). Thus, it is likely that the campus will be subjected to large ground motions generated by future large earthquakes on the active faults in the region.

The fault model used in this study is adopted from a model developed by Wong *et al*. (2008b). Each seismic source is characterized using the latest available geologic, seismologic, and paleoseismic data and the currently accepted models of fault behavior developed by the Working Group on Northern California Earthquake Potential (WGNCEP, 1996) and the 2002 California Geological Survey's

(CGS) seismic source model used in the USGS National Hazard Maps (Cao *et al.*, 2003). Characterizations of the major faults in the San Francisco Bay region, the San Andreas, Hayward/Rodgers Creek, Concord/Green Valley, San Gregorio, Greenville, and Mt. Diablo thrust faults, are adopted from the 1999 and 2002 Working Groups on California Earthquake Probabilities (WGCEP, 2003). Characterization of other faults not considered by these other sources (e.g., Stanford fault) was performed as part of this study.

Figs. 1 and 2 show the locations of the faults relative to campus. Faults are included that are judged to be at least potentially active and that may contribute to the probabilistic hazard because of their maximum earthquakes and/or proximity to the campus. In this analysis, most faults are modeled as single, independent, planar sources extending the full extent of the seismogenic crust. Thus, fault dips are averages estimated through the seismogenic crust. Generally, in western California, the seismogenic crust ranges from 11 to 15 km thick based on well-located contemporary seismicity (e.g., Oppenheimer and MacGregor-Scott, 1992). Fault zones are modeled as multiple, parallel planes within the zone boundaries (e.g., Briones zone).

Recurrence rates for many of the faults within the San Francisco Bay region are either poorly understood or unknown due to a lack of reliable paleoseismic data. Thus, we express fault activity as an average annual slip rate (in mm/yr) rather than recurrence intervals (years between events). The uncertainty in slip rates and other input parameters are accommodated in the PSHA through the use of logic trees.

Uncertainties in determining recurrence models can significantly impact the hazard analysis. We consider truncated exponential, maximum-magnitude, and characteristic recurrence models, with various weights depending on source geometry and type of rupture model. Historical seismicity and paleoseismic investigations along faults in the western U.S. (e.g., San Andreas fault) suggest that characteristic behavior is more likely for individual faults (Schwartz and Coppersmith, 1984). Therefore, we generally favor the characteristic model for all fault sources (weight of 0.70) while the maximum magnitude model is weighted 0.30.

Of particular relevance to the campus is the Stanford fault zone. The fault zone comprises several northwest-striking, west-dipping, left-stepping *en echelon* oblique-reverse faults at the northern end of the Foothills thrust belt, east of the San Andreas fault, that links the San Andreas and Monte Vista faults (Fenton and Hitchcock, 2001; Angell *et al.*, 1998). It is considered to be a blind fault, underlying the Stock Farm monocline on campus, that has caused warping of Plio-Pleistocene and younger deposits (Fenton and Hitchcock, 2001). Although the Stanford fault has clear evidence of latest Pleistocene to Holocene deformation, given the observations of Hitchcock and Kelson (1999), we consider the possibility that the fault does not act as an independent seismogenic source, but only ruptures in conjunction with the San Andreas fault in triggered slip events. There is no conclusive evidence, given that higher triggered slip around the Stanford fault was not reported following the Loma Prieta earthquake, that all the slip on the Stanford fault occurs in triggered slip events, although some of it may. Modeling by Angell *et al* (1998) suggests the Stanford fault merges with the San Andreas fault below about 10 km depth, well within the range of earthquake nucleation. Thus the fault is large and deep enough to generate surface deforming earthquakes without being triggered by another fault. Given these considerations, we assigned a probability of 0.7 that the Stanford fault is an independent active seismic source. The slip rate for the Stanford fault of 0.4 to 1.0 mm/yr was adopted from Bullard *et al*. (2004) who measured vertical displacements of Quaternary terraces across the fault.

The probabilistic hazard was calculated using the PEER Next Generation of Attenuation (NGA) models. These models included Abrahamson and Silva (2008), Boore and Atkinson (2008), Campbell and Bozorgnia (2008), and Chiou and Youngs (2008). All models were equally weighted. The relationship by Idriss (2008) was not used because it did not include soil site conditions. The hazard was calculated at two sites corresponding to locations within the north-central and east campus, Roble Field and the Stadium, respectively (Fig. 4).

A V_S30 of 270 m/sec, which is an average value for generic firm soil, was used in the PSHA and deterministic calculations. This value was selected because it is well represented in the NGA strong motion database. The resulting firm soil hazard is then adjusted for the site-specific site conditions using the base case V_S profiles in the site response analysis.

Other NGA input parameters include $Z_{1.0}$, the depth to a V_S of 1.0 km/sec used only by Abrahamson and Silva (2008) and Campbell and Bozorgnia (2008) and $Z_{2.5}$, the depth to a V_S of 2.5 km/sec, which is only used in one model, Campbell and Bozorgnia (2008). Both parameters were used by the model developers to approximate basin effects. We have used the default values as recommended by the authors. In the absence of site-specific data, the authors provide an equation for default values based on the V_S30 at the site. Other parameters such as depth to the top of rupture (zero for all surficial faults unless specified otherwise), dip angle, and rupture width are specified for each fault or calculated within the PSHA code. Fault rupture directivity as modeled by Somerville *et al.* (1997) and modified by Abrahamson (2000) is incorporated into the PSHA results. The PSHA results are calculated for the fault-average component.

The probabilistic hazard at the Stanford campus is controlled by the San Andreas fault at almost all return periods and spectral periods. Although the Stanford fault underlies the campus, its comparatively lower slip rate (0.4-1.0 mm/yr) and lower probability of activity (0.7) results in only a small contribution to the probabilistic hazard.

Horizontal Uniform Hazard Spectra (UHS) for return periods of 475 and 2,475 years (10% and 2% exceedance probabilities in 50 years, respectively) are shown on Fig. 6 for the two campus areas. The generic firm soil ground motions are slightly higher for the north-central campus as compared to east campus simply because the north-central campus is closer to the San Andreas fault, the controlling seismic source in the probabilistic hazard.

DETERMINISTIC SEISMIC HAZARD ANALYSIS

Five percent-damped 84th-percentile horizontal acceleration response spectra were calculated for the maximum earthquake on the San Andreas fault (**M** 7.9) at source-to-site distances of 6.5 km from north-central campus (Roble Field) and 8.1 km from east campus (Stadium) using the same NGA relationships used in the PSHA.

Figure 6 also shows comparisons of the deterministic spectra with the 475 and 2,475-year return period UHS. The deterministic spectra were not adjusted for fault rupture directivity at the recommendation of the Stanford Ground Motion Review Committee because it was believed that the use of the 84th-percentile spectrum was adequately conservative to account for rupture directivity. The north-central campus spectra both deterministic and UHS are higher as expected than the east campus spectra (Fig. 6). The 84th percentile deterministic spectra are similar to the 475-year return period UHS except at spectral periods longer than about 0.3 sec where they become higher.

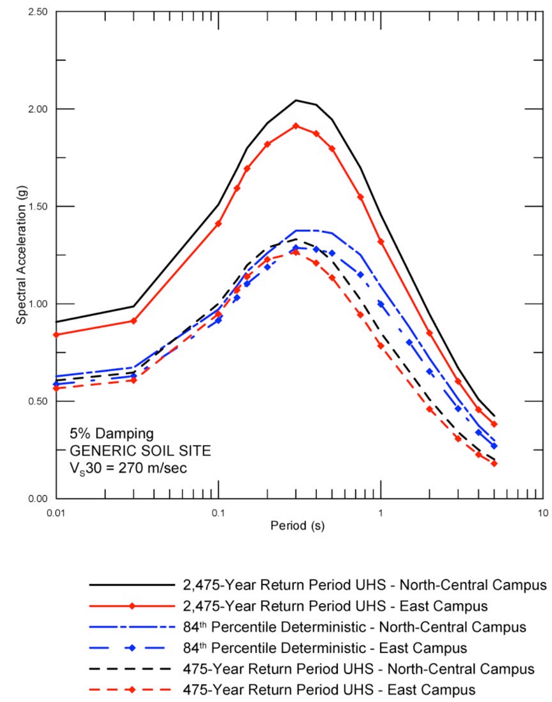

Fig. 6. Comparison of UHS at 475- and 2,475-yr return periods and 84th percentile deterministic spectra for north-central and east campus.

SITE RESPONSE ANALYSIS

A site response analysis was performed using the approach of McGuire *et al*. (2001) and Bazzurro and Cornell (2004). In this approach, the hazard at the soil surface is computed by integrating the site-specific hazard curves at a generic rock or soil level with the probability distribution of the amplification function. Amplification factors were computed using random vibration theory (RVT) (Silva and Lee, 1987). In this approach, as embodied in the computer program RASCALS, the control motion power spectrum is propagated through the 1-D soil profile. To perform the site response analysis, representative base case V_S profiles of the site, previously described, and shear modulus (G/Gmax) reduction and damping curves are required. For the dynamic material properties, the EPRI (1993) sand curves and Peninsular Range curves (Silva *et al.*, 1997) were used to cover the range of nonlinear behavior at the site. The two dynamic material models were weighted equally when combining the site response analyses results obtained from the two velocity models.

To randomly vary the base case V_S profile, a profile randomization scheme based on a correlation model was used (Silva *et al.*, 1997). Profile depth (depth to competent material) is also varied on a site-specific basis using a uniform distribution. The depth range is generally selected to reflect expected variability over the structural foundation as well as uncertainty in the estimation of depth to competent material. To accommodate variability in shear modulus reduction and hysteretic damping curves on a generic basis, the curves are independently randomized about the base case values. A lognormal distribution is assumed with a σ_{ln} of 0.35 at a cyclic shear strain of 3×10^{-2} %.

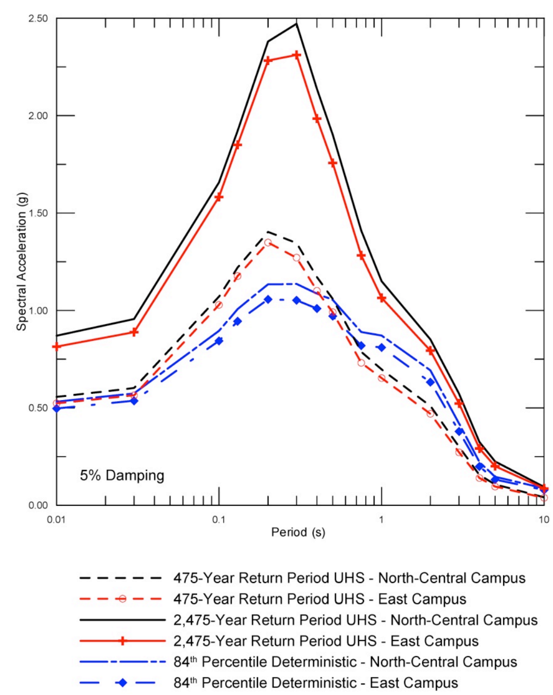

Fig. 7. Comparison of site-specific UHS at 475- and 2,475-yr return periods and 84th percentile deterministic spectra for north-central and east campus.

For the two base case V_S profiles, north-central campus and east campus, 30 randomized V_S profiles were generated. Associated with each 30 randomized profile was a set of randomized dynamic material property curves. Based on RASCALS runs for the 30 V_S profiles for each base case, a probability

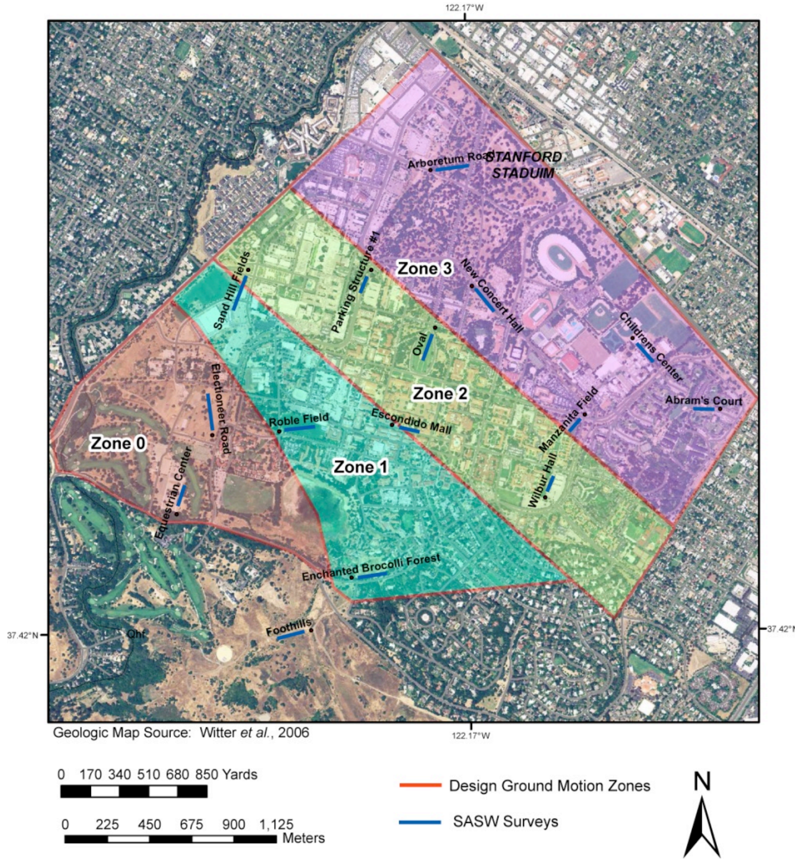

Fig. 8. Design ground motion zones and SASW survey locations.

distribution of amplification factors was calculated. The suite of amplification factors with respect to generic firm soil (V_S30 of 270 m/sec) were applied to the generic soil hazard curves. From these amplified curves, hazard-consistent site-specific UHS were calculated for return periods of 475 and 2,475 years for the north-central and east campuses (Fig. 7).

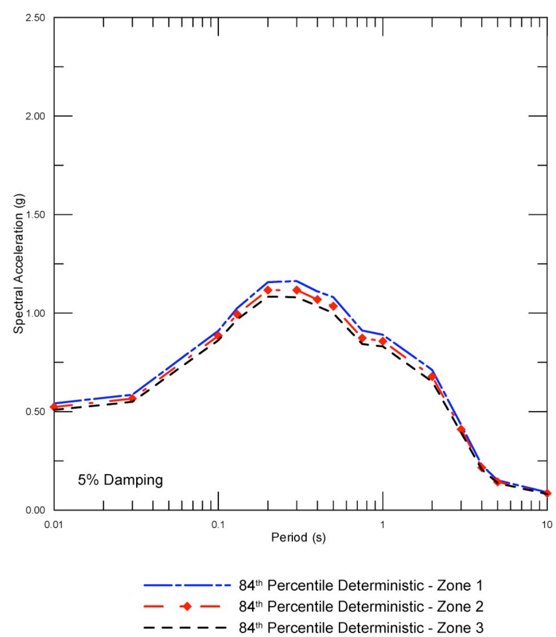

Fig. 9. Comparison of 84th percentile site-specific deterministic spectra for Zones 1, 2, an 3.

The median amplification factors were applied to the median horizontal acceleration response spectra for the **M** 7.9 San Andreas maximum earthquake (V_S30 of 270 m/sec) to arrive at the median deterministic site-specific spectra for the north-central and east campuses. The 84th-percentile spectra were then calculated using the aleatory sigma from each of the four NGA models (Fig. 7). Figure 7 compares site-specific UHS and 84th percentile **M** 7.9 deterministic spectra that incorporate site effects for both north-central and east campus.

Note that these surface spectra exhibit the unsmoothed characteristics of spectra derived from actual strong motion data. In this case, the bump in the spectra centered at about 1.5 sec is probably due to modeling the soil/rock contrast at varying depths. Given the absence of data on the depth of this contact, the bump is probably broader than what would be observed in actual strong motion data.

Following earlier discussions with the Ground Motion Review Committee, it was decided to attempt to microzone the campus because the range of preliminary design ground motions was relatively large. Thus the campus was zoned into four zones based on ground motion characterization (Fig. 8). Design ground motions for the entire campus area are controlled by the deterministic ground motions (**M** 7.9 on the nearby San Andreas fault). These motions decrease as the distance from the fault increases across campus from the southwest to the northeast, which controls the orientation of the three zones shown on Fig. 8. Given the similarities in base case V_S profiles, site response effects are not significantly different in the campus microzonation except at long periods. Zone 0 is the west campus with relatively thin soil of variable thickness over rock where site-specific studies will be required (Fig. 8).

For zones 1 to 3, site-specific median and 84th percentile deterministic spectra were computed (Fig. 9). The 84th percentile deterministic spectra are similar given the similarity in the distances to the San Andreas fault. Zone 1 has the slightly higher ground motions since it is closest to the fault. Probabilistic spectra (2,475-yr and 475-year UHS) were not recomputed for the zones because the deterministic ground motions control the design motions for all locations on campus, i.e., they are lower.

DESIGN RESPONSE SPECTRA

Design ground motions for the three zones were computed following both ASCE 7-05 and ASCE 41-06, resulting in Maximum Considered Earthquake (MCE) and DRS (ASCE 7-05) and BSE-2 and BSE-1 spectra (ASCE 41-06) for each zone except for Zone 0.

MCE and DRS

As defined by ASCE 7-05, the site-specific MCE is the lower of the site-specific probabilistic (2,475-year UHS) and site-specific deterministic spectrum. Also the site-specific deterministic spectrum must not be below a code-defined minimum deterministic spectrum. Figure 10 illustrates the development of the site-specific MCE for Zone 1. The site-specific deterministic spectrum (84th percentile) is first compared to the ASCE 7-05 lower limit for site-specific deterministic spectra. (Note that both ASCE 7-05 and ASCE 41-06 call for the site-specific deterministic spectrum to be 1.5 times the site-specific median spectrum. We have replaced this approach using the 84th percentile spectrum as appears in ASCE 7-10.) The lower limit is determined from the code for both NEHRP site classes C and D due to the variation of soils within Zone 1. The lower limit exceeds the site-specific deterministic spectrum except at periods of about 1 to 4 sec. The envelope of these spectra is the deterministic MCE spectrum per ASCE 7-05.

Figure 11 shows the development of the site-specific MCE using the same process with the additional step of computing the maximum-rotated spectrum for both the deterministic and probabilistic site-specific spectra. The maximum-rotated component spectra are computed by applying the factors developed by Huang *et al*. (2008). These period-dependent factors reflect the ratio of the maximum spectral acceleration to the geometric mean spectral acceleration at each period. The maximum component MCE is provided here as a comparison. Currently, ASCE 7-05 and ASCE 41-06 do not require the use of maximum component spectra. Although, the use of the maximum component is now described in the recently developed ASCE 7-10, its use is not yet required in design of buildings except for hospitals.

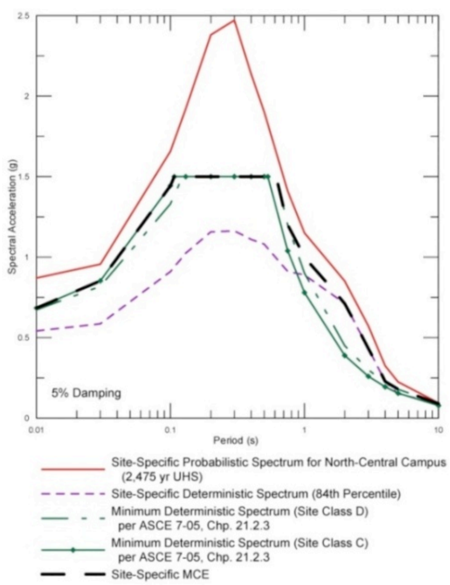

Fig. 10. Site-specific MCE compared to probabilistic and deterministic spectra for Zone 1.

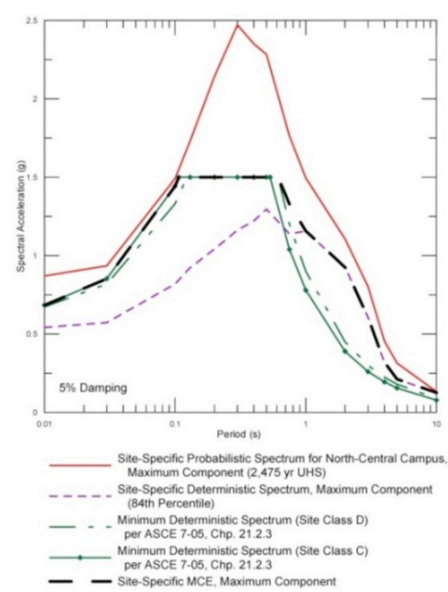

Fig. 11. Site-specific maximum component MCE compared to probabilistic and deterministic spectra for Zone 1.

In Fig. 12, two-thirds of the site-specific MCE is compared with the lower limit of 80% of the ASCE 7-05 code general DRS for site classes C and D. The two-thirds site-specific MCE is lower than the 80% ASCE 7-05 general DRS for site classes C and D except in the period range of about 1 to 4 sec, so the envelop of the spectra is the site-specific DRS for Zone 1. Figure 13 illustrates the site-specific DRS using the maximum rotated component spectra. The use of the maximum component would result in higher design ground motions at spectral periods of 0.7 to 5 sec.

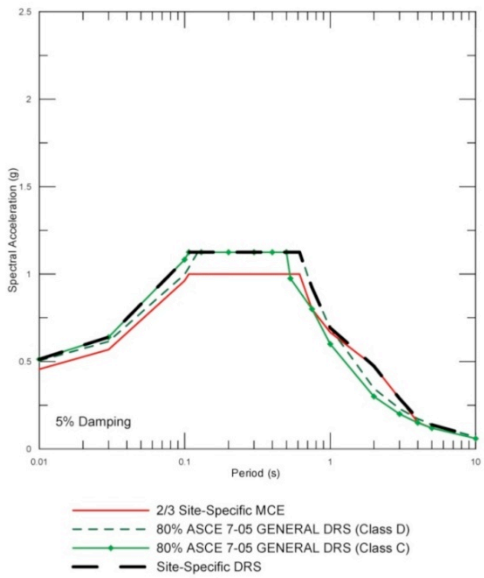

Fig. 12. Site-specific DRS for Zone 1.

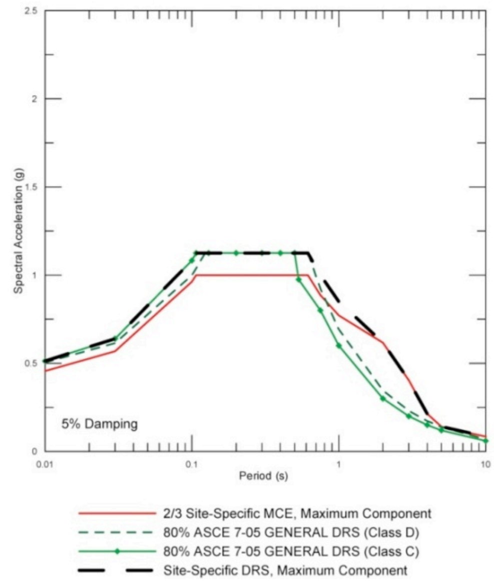

Fig. 13. Site-specific maximum component DRS or Zone 1.

MCE and DRS are developed following the above process for Zones 2 and 3. Figure 14 summarizes the site-specific MCE and DRS for the three zones. Due to the lower limit deterministic spectrum of ASCE 7-05 controlling most of the MCE spectra, there is little difference between the MCE for the three zones. However, the DRS are controlled by the general code minimum and so there are small differences between the zone spectra. Figure 15 summarizes the site-specific MCE and DRS using the maximum-rotated component spectra. The maximum-rotated component spectra are larger only at periods greater than 0.8 sec due to the code minimums controlling the spectra.

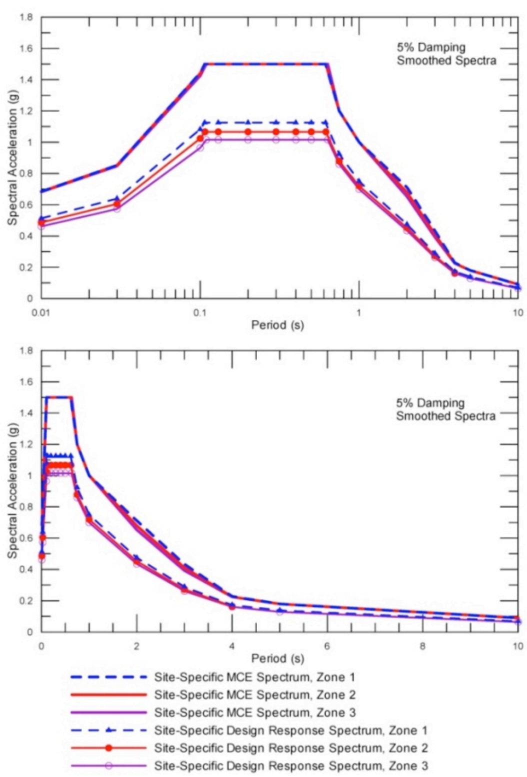

Fig. 14. Site-specific MCE and DRS for Zones 1, 2, and 3.

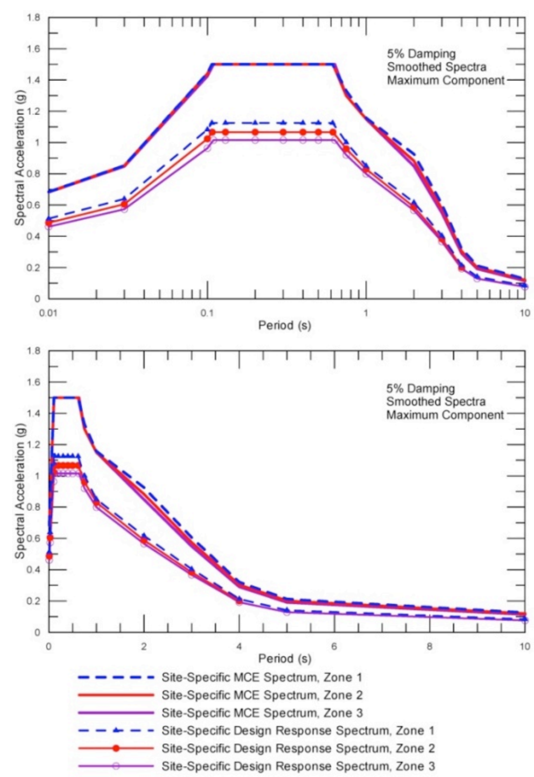

Fig. 15. Site-specific maximum component MCE and DRS for Zones 1, 2, and 3.

BSE-2 and BSE-1 Spectra per ASCE 41-06

According to ASCE 41-05, the site-specific BSE-2 is the lower of the site-specific 2,475-year UHS and the site-specific deterministic spectrum. The site-specific BSE-1 spectrum is the lower of two-thirds of the site-specific BSE-2 spectrum and the site-specific 475-year UHS. In addition, the site-specific BSE-2 and BSE-1 must not be lower than 70% of the ASCE 41-06 general BSE-2 and BSE-1. These spectra are shown on Fig. 16 for all zones. The deterministic (84th percentile) spectrum is lower than the 2,475-year UHS at all periods. The lower limit of 70% of the general code spectrum controls the site-specific BSE-2 spectrum at all periods less than about 1 sec. Figure 17 illustrates the site-specific BSE-2 and BSE-1 spectra for all zones using the maximum-rotated component spectra. The maximum component-based BSE-2 spectrum is higher than the geomean-based BSE-2 spectrum beyond 0.7 sec.

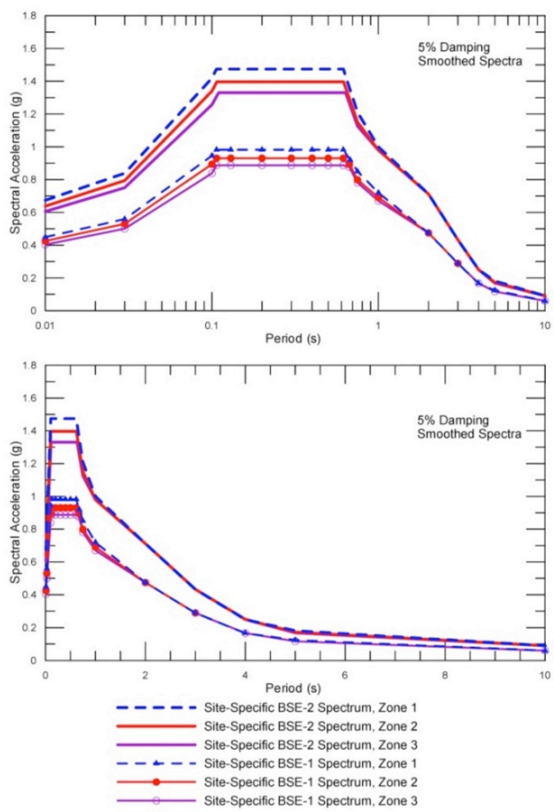

Fig. 16. Site-specific BSE-1 and BSE-2 response spectra for Zones 1, 2, and 3.

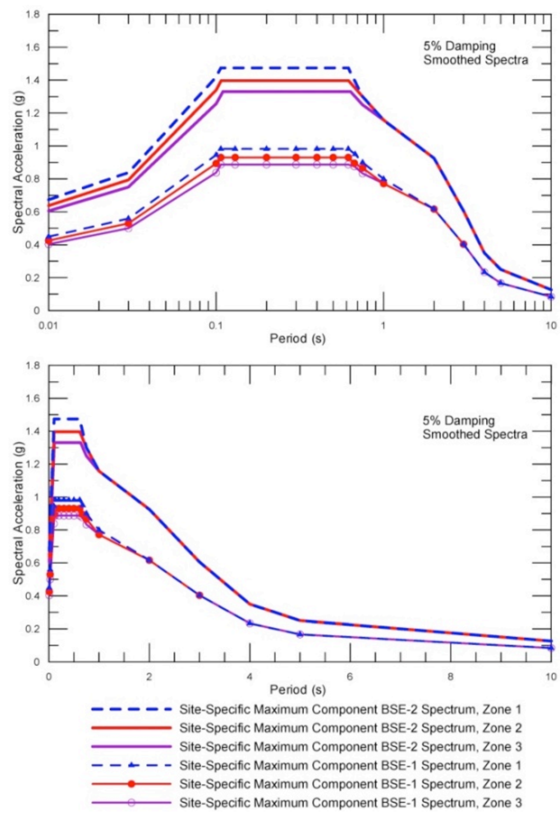

Fig. 17. Site-specific maximum component BSE-1 and BSE-2 response spectra for Zones 1, 2, and 3.

CONCLUSIONS

A seismic hazard evaluation was updated and design ground motions developed for the Stanford University campus. Due to a lack of site-specific velocity data for the campus, the earlier 2008 ground motions incorporated a large measure of epistemic uncertainty in the V_S profiles and thus were probably too conservative. To address this issue, V_S measurements were made at 15 locations across campus using the SASW method. The V_S data was used to define preliminary areas of the campus (north-central and east) with separate base case velocity profiles for site response analyses. The west campus was identified based on the SASW surveys as an area that will require site-specific analyses because of its thin soil characteristics.

One-dimensional site-response analyses were performed for both north-central and east campus areas using the 475-year and 2,475-year return periods UHS and the 84th percentile deterministic spectra for a firm soil site condition as input ground motions. Resulting surface ground motions are the basis for the development of design ground motions following both ASCE 7-05 and ASCE 41-06 procedures.

Due to the range of design ground motions, it was decided to further microzone the campus. Following the procedures and requirements of ASCE 7-05 and ASCE 41-06, the design ground motions are controlled by the deterministic event, a **M** 7.9 earthquake on the nearby San Andreas fault. The ground motion hazard is a function of the distance to the fault and site response at long periods; hence the orientation of the three final zones is essentially parallel to the San Andreas fault. The width of the zones is a result of the ground motion level and the expected future building construction on campus.

BSE-1 and BSE-2 spectra and DRS were developed in this study for Stanford University consistent with the standards ASCE 41-06, ASCE 7-05, and ASCE 7-10. Spectra were calculated using the geomean ground motions per ASCE 7-05 and the maximum-rotated ground motions per ASCE 7-10. This range of design ground motions can be used for both new and existing buildings. The decision on the application of all or some of these spectra rests with the University.

The use of the maximum-rotated component as described in ASCE 7-10, but not in the current ASCE 7-05 or ASCE 41-06 guidelines, is not currently being used in design with the exception of hospitals and other structures subject to the requirements of the Office of Statewide Health Planning and Development (OSHPD). Thus a decision will be required by Stanford University on whether the maximum-component ground motions should be used as the basis for design for the DRS as well as BSE-1 and BSE-2 spectra. We expect that the use of maximum component will be incorporated into practice once the next version of the IBC is completed. For existing buildings, we do not know when the maximum component will be incorporated into ASCE 41.

ACKNOWLEDGMENTS

This project was supported by Stanford University. Our thanks to Jean Barnes, Eoin Buckley, and Jay Marianowits for their support and assistance in this study. Thanks also to Laura Hansen, Judy Zachariasen, and Melinda Lee who assisted in the study and preparation of the report, to Laura Knutson for discussions on the campus geology, Cecil Hoffpauir and Chang Young Kim for their assistance in the SASW surveys, and Bob Green for his review of the report. Special thanks to NEES.com for shared-use status of the mobile vibrators. Our thanks also to the Stanford Ground Motion Review Committee, which consists of Charlie Kircher, Bill Holmes, Ron Hamburger, Greg Deierlien, Harry Jones, and Fouad Bendimerad.

REFERENCES

Abrahamson, N. [2000]. "Effects of Rupture Directivity on Probabilistic Seismic Hazard Analysis", *Proc. Sixth Intern. Conf. on Seismic Zonation*, Vol. I, p. 151-156.

Abrahamson, N.A., and W.J. Silva [2008]. "Summary of the Abrahamson and Silva NGA Ground Motion Relations", Earthquake Spectra, Vol. 24, pp. 67-97.

Angell, M.A., K.L. Hanson, and T. Crampton [1998]. "Characterization of Quaternary Contractional Deformation Adjacent to the San Andreas Fault, Palo Alto, California", Final Report submitted to the U.S. Geological Survey, National Earthquake Hazards Reduction Program, Award No. 1434-95-G-2586.

Bazzurro, P., and C.A. Cornell [2004]. Nonlinear Soil-Site Effects in Probabilistic Seismic-Hazard Analysis", Bull. Seis. Soc. Am., Vol. 94, pp. 2110-2123.

Boore, D.M., and G.M. Atkinson [2008]. "Ground Motion Predictive Equations for the Average Horizontal Component of PGA, PGV, and 5% Damped PSA at Spectral Periods Between 0.01s to 10.0s", Earthquake Spectra, Vol. 24, pp. 99-138.

Bullard, T.F., K.L. Hanson, and H.F. Abramson-Ward [2004]. "Quaternary Investigations to Evaluate Seismic Source Characteristics of the Frontal Thrust Belt, Palo Alto Region, California", Final Report to U.S. Geological Survey, National Earthquake Hazards Reduction Program, Awards 01HQGR0015 and 01HQCR0016.

Campbell, K.W., and Y. Bozorgnia [2008]. "NGA Ground Motion Model for the Geometric Mean Horizontal Component of PGA, PGV, PGD, and 5% Damped Linear Elastic Response Spectra for Periods Ranging From 0.01 to 105", Earthquake Spectra, Vol. 24, pp. 139-171.

Cao, T., W.A. Bryant, B. Rowshandel, D. Branum, C.J. Wills [2003]. "The Revised 2002 California Probabilistic Seismic Hazard Maps, June 2003", California Geological Survey, http://www.consrv.ca.gov/CGS/rghm/psha/fault_parameters/pdf/2002_CA_Hazard_Maps.pdf.

Chiou, B.S.J., and R.R. Youngs [2008]. "An NGA Model for the Average Horizontal Component of Peak Ground Motion and Response Spectra", Earthquake Spectra, Vol. 24, pp. 173-215.

Cornell, C.A. [1968]. "Engineering Seismic Risk Analysis", Bull. Seis. Soc. Am., Vol. 58, pp. 1583-1606.

Electric Power Research Institute (EPRI) [1993]. "Guidelines for Determining Design Basic Ground Motions, v. 1: Method and Guidelines for Estimating Earthquakes Ground Motion in Eastern North America", EPRI Report TR-102293.

Fenton, C.H., and C.S. Hitchcock [2001]. "Recent Geomorphic and Paleoseismic Investigations of Thrust Faults in Santa Clara Valley, California in Engineering Geology Practice in Northern California", Association of Engineering Geologists Special Publication 12, Edited by H. Ferriz and R. Anderson, pp. 239-257.

Hitchcock, C., and K. Kelson [1999]. "Growth of Late Quaternary Folds in Southwest Santa Clara Valley, San Francisco Bay Area, California: Implications of Triggered Slip for Seismic Hazard and Earthquake Recurrence", Geology, Vol. 27, pp. 391–394.

Huang, Y., A.S. Whittaker, and N. Luco [2008]. "Maximum Spectral Demands in the Near-Fault Region", Earthquake Spectra, Vol. 24, pp. 319-341.

Idriss, I.M. [2008]. "An NGA Empirical Model for Estimating the Horizontal Spectral Values Generated by Shallow Crustal Earthquakes", Earthquake Spectra, Vol. 24, pp. 217-242.

McGuire, R.K., W.J. Silva, and C.J. Costantino [2001]. "Technical Basis for Revision of Regulatory Guidance on Design Ground Motions: Hazard- and Risk-Consistent Ground Motion Spectra Guidelines", U.S. Nuclear Regulatory Commission NUREG/CR-6728.

Oppenheimer, D.H., and N. Macgregor-Scott [1992]. "The Seismotectonics of the Eastern San Francisco Bay Region," in G. Borchardt, S.E. Hirschfeld, J.J. Lienkaemper, P. McClellan, P.L. Williams, and I.G. Wong (eds.), *Proceedings of the Second Conference on Earthquake Hazards in the Eastern San Francisco Bay Area*, California Division of Mines and Geology Special Publication 113, pp. 11-16.

Schwartz, D.P., and K.J. Coppersmith [1984]. "Fault Behavior and Characteristic Earthquakes--Examples From the Wasatch and San Andreas Fault Zones", Jour. Geotech. Res., Vol. 89, pp. 5681-5698.

Silva, W.J., N.A. Abrahamson, G. Toro, and C. Constantino [1997]. "Description and Validation of the Stochastic Ground Motion Model", unpublished report prepared for the Brookhaven National Laboratory.

Silva, W.J., and K. Lee [1987]. "WES RASCAL Code for Synthesizing Earthquake Ground Motions, State-of-the-Art for Assessing Earthquake Hazards in the United States", Report 24, U.S. Corps of Engineers Waterways Experiment Station, Miscellaneous Paper S-73-1, 120 p.

Somerville, P.G., N.F. Smith, R.W. Graves, and N.A. Abrahamson [1997]. "Modification of Empirical Strong Ground Motion Attenuation Relations to Include the Amplitude and Duration Effects of Rupture Directivity", Seis. Res. Let., Vol. 68, pp. 199-222.

Stokoe, K.H., II, S.G. Wright, J.A. Bay and, and J.M. Roesset [1994]. "Characterization of Geotechnical Sites by SASW Method", ISSMFE Technical Committee 10 for XIII ICSMFE, Geophysical Characteristics of Sites, pp. 795-816.

Thomas, P.A., I.G. Wong, and N. Abrahamson [2010]. "Verification of Probabilistic Seismic Hazard Analysis Software Programs", PEER Report 2010/106, Pacific Earthquake Engineering Research Center, College of Engineering, University of California, Berkeley, 173 p.

Witter, R.C., K.L. Kundsen, J.M. Sowers, C.M. Wentworth, R.D. Koehler, and C.E. Randolph [2006]. "Maps of Quaternary Deposits and Liquefaction Susceptibility in the Central San Francisco Bay Region, California, Part 3: Description of Mapping and Liquefaction Interpretation", U.S. Geological Survey Open-File Report 2006-1037.

Wong, I., P. Thomas, L. Hansen, W. Silva, N. Gregor, K. Stokoe, and J. Yuan [2008a]. "Update to the Site-Specific Seismic Hazard Analyses and Development of Seismic Design Ground Motions, Stanford University, California", unpublished report prepared for Stanford University.

Wong, I., P. Thomas, J. Unruh, K. Hanson, and R. Youngs [2008b]. "Characterizing the Earthquake Ground Shaking Hazard in the Sacramento-San Joaquin Delta, California", *Geotechnical Earthquake Engineering and Soil Dynamics Conference, IV Proceedings* (CD ROM).

Working Group on Northern California Earthquake Potential (WGNCEP) [1996]. "Database of Potential Sources for Earthquakes Larger than Magnitude 6 in Northern California", U.S. Geological Survey Open-File Report 96-705, 53 p.

Working Group for California Earthquake Probabilities (WGCEP) [2003]. "Earthquake Probabilities in the San Francisco Bay Area: 2002-2031", U.S. Geological Survey Open-File Report 03-214.